"***A Review and Update of Mantle Thermobarometry for Primitive Arc Magmas***" Electronic Supplementary Material

C.B. Till

1. Reverse Fractional Crystallization Calculation Methodology

To obtain the P-T conditions of mantle partial melting, a primitive melt inclusion, bulk rock or matrix glass composition first must be adjusted for crystal fractionation. The various considerations required in these calculations, such as the mantle olivine composition, the choice of fractionating minerals and the equilibrium mantle residue assemblage (lherzolite, harzburgite or dunite) are discussed below.

a) Mantle Olivine Composition

The most common practice is to conduct reverse fractional crystallization calculations for primitive magmas until the liquid is in equilibrium with a designated mantle olivine composition, typically an olivine composed of 90-91% forsterite (Fo90-91), using an olivine-liquid partitioning coefficient model such as Herzberg and Asimow (2008) or Putirka (2016) or a constant olivine-liquid Fe-Mg K_D of 0.3 (e.g., Roeder and Emslie 1970). The choice of olivine forsterite content chosen for the mantle residue can have a significant effect on the composition of the fractionation corrected liquid and thus the calculated temperature and pressure of origin. For example, when a high-alumina olivine tholeiite (HAOT) typical of dry primitive arc magmas is corrected back to equilibrium with Fo90 mantle olivine, the liquid yields a temperature estimate that is 40°C lower than the liquid in equilibrium with a Fo91 mantle olivine using the thermometer of Sugawara (2000). Pressure estimates for this composition are up to 4 kbar lower

for a liquid in equilibrium with Fo90 olivine relative to Fo91 using the Albaréde (1992) barometer with the correction of Leeman et al. (2005).

Putirka (2016) recently demonstrated that the model chosen for olivine-liquid Fe-Mg K_D (Roeder and Emslie 1970; Toplis, 2005; Matzen et al., 2011), as well as that for the effect of liquid X_{Fe2O3}/X_{FeO} on olivine-liquid Fe-Mg K_D is another important consideration that will affect the resulting liquid composition and calculated temperatures (see Putirka 2016 Fig. 3). In particular, the models of Kress and Carmichael (1991) and Jayasuriya et al. (2004) predict large changes in liquid X_{Fe2O3}/X_{FeO} as a function of liquid temperature, whereas Kress and Carmichael (1988) and Putirka (2016) equation 6b show little to no variation as a function of temperature alone. Using models with a larger dependence of liquid X_{Fe2O3}/X_{FeO} on temperature would cause studies that approximate all Fe as FeO* (as is done here for the recalculated P & T in Section 3) to overpredict the temperatures compiled in Figure 1 of the main text (i.e., in the most extreme models, an increase in liquid X_{Fe2O3}/X_{FeO} =0.1 results in a decrease in the mantle equilibration temperature of up to 150°C). This effect on the mantle-melt thermometry is similar to adding ~5 wt% H_2O to a liquid previously assumed to be dry, reinforcing the importance of considering both fO_2 and H_2O in reconstructing arc magma mantle pressure-temperatures. If the models where Fe_2O_3 plays an important role in mantle equilibration temperature are correct, then it suggests arc magmas with significant Fe_2O_3 are shifted to lower temperatures at upper mantle wedge pressures. This strengthens the conclusions that these melts re-equilibrate with the mantle as they rise though the wedge, such that they can record the lower temperatures in the top half of the mantle wedge (i.e., experience reactive porous flow), and does not change the genetic interpretations of the different primary arc magma types presented in Section 4.4.

b) Choice of Mantle Residue

Exhumed mantle sections, xenoliths and an abundance of petrologic studies suggest lherzolite, harzburgite and dunite lithologies are all found in the sub-arc mantle (e.g., Pearce and Parkinson 1993; Kelemen et al., 1995a; Morishita et al. 2011; Pirard et al. 2013). Thus primitive arc liquids may be generated from any of these and/or re-equilibrate with them en route to the surface. Thus calculations to return a liquid to equilibrium with the mantle need to consider which of these lithologies is most likely, as the choice will alter the target composition for the reverse fractionation calculation, in addition to providing insight into the magma's origin. The composition of liquids in equilibrium with lherzolite (e.g., Green 1987; Mysen and Boettcher 1975; Till et al. 2012; Grove et al. 2013) and harzburgite (Umino and Kushiro 1989; Falloon and Danyushevsky 2000; Mitchell and Grove, 2015; Mitchell and Grove, 2016) have been experimentally studied, such that models for their melting exist and liquids can be plotted in pseudo-ternary projections and on other geochemical discrimination diagrams to assess the appropriate mantle residue. Figure 4 in the main text illustrates the composition of primitive liquids prior to fractional crystallization correction that were previously in equilibrium with lherzolite (Fig. 4a) and harzburgite (Fig. 4b and c) when plotted on a Plag-Oliv-Qtz pseudo-ternary diagram projected through clinopyroxene. Multiple other projections for these same liquids are included here in Figure S1 along with a summary figure in Figure S2 to help guide choices of potential residues for a given sample. Reaction with dunite residues have also been studied experimentally (e.g., Kelemen et al. 1995; Pirard and Hermann, 2015; Wang et al. 2016; Mitchell and Grove, 2016). Liquids that reacted with dunite residues en route to the surface may be harder to distinguish from harzburgite residues, as they will gain or lose olivine depending on the particular ambient pressure-temperature conditions and the magma flux but the dunite bodies are not substantially diverse in Mg#, so those liquids will not change their Mg#'s. Thus these

liquids may be shifted toward or away from the Olivine apex of normative projections without large changes in Mg#, as would occur during fractional crystallization of olivine. Projections through the Olivine component that compare reverse-fractionated liquids with lherzolite and harzburgite multiple saturation points may be the best way to assess such liquids.

c) Choice of Fractionating Minerals for Reverse Fractional Crystallization Calculation

The choice of fractionating minerals utilized in the reverse fractionation calculation will affect the composition of the remaining liquid and thus the resulting pressure and temperature calculations. The fractional crystallization paths of mid-ocean ridge basalts (MORB) have been well established through experimental and petrologic studies (e.g., Tormey et al. 1987; Grove et al. 1992; Yang et al. 1996). MORBs tend to fractionate olivine and plagioclase and the critical variable in reconstructing fractionation paths is pressure. Calculations to adjust for fractional crystallization become more complex for primitive arc magmas and other primitive magmas erupted in continental settings, as their phase assemblages and sequences of crystallization are dependent on other variables besides pressure. The key is to have a set of lavas related by fractional crystallization that can be used to identify 1) the proportion of the phases that crystallized, 2) the degree of crystallization of the magma with a given phase assemblage, and if applicable 3) the switching point between sets of co-crystallizing phase assemblages (i.e., when the magma leaves a cotectic). If a suite of samples related by crystallization are not available, this process can be applied using the mineral assemblage and chemistry from a single sample to try and reconstruct the fractionation path until the corrected liquid is in equilibrium with mantle olivine and plots on a mantle multiple saturation point, although the path may be harder to discern. This can process can be visualized on the ternary diagram in Figure 4 in the main text (also see worked example below). This method provides a rigorous approach to return a liquid

with multiphase fractionation to its primary composition. An alternative approach is to restrict thermometry and barometry to primitive samples that have experienced a minimal amount of crystal fractionation, such that they have only experienced olivine crystallization, which is more straightforward to correct for.

The choice and composition of fractionating phases can also be guided by experimental studies of the liquid line of descent for primitive arc magmas. These experimental studies essentially examine of three different bulk compositions: 1) low MgO high Al_2O_3 basalts (e.g., Sisson and Grove 1993a; Wagner et al. 1995; Tatsumi and Suzuki 2009), 2) High MgO basalts (e.g., Parman et al. 2011; Blatter et al. 2013; Hamada and Fujii 2008), and 3) basaltic andesites and andesites (e.g., Grove et al. 2003; Mandler et al. 2014). The resulting effect of the crystallizing assemblage can be visualized in Figure S3 (and Fig. 3 of the main text). Together these studies illustrate that increasing the water contents or fO_2 at a constant pressure will cause the temperature of plagioclase crystallization to go down relative to the liquidus, thereby reducing the proportion of plagioclase crystallized compared to the ferromagnesian silicates and increasing the SiO_2 content of the residual liquid. These studies also find that the crystallization calcic plagioclase (>An90) results from high H_2O contents and cannot form from dry melts with normal arc Na_2O and CaO as first demonstrated by Sisson and Grove (1993a). Blatter et al. (2013) focus on the crystallization pathways of a relatively magnesian basalt (8.7 wt% MgO) typical of mafic magmas erupted in the Cascades near Mt. Rainer, Washington over a range of crustal pressures. Experiments were conducted with 2 wt% H_2O at 900, 700 and 400 MPa. Clinopyroxene is the first phase to crystallize at 900 and 700 MPa, and there is a broad interval of augite + olivine + orthopyroxene + Cr-spinel (in order of decreasing abundance) until at lower temperatures plagioclase and Fe-Ti oxides replace spinel, and then olivine. The lowest pressure

liquids (the most calc-alkaline) exhibit plagioclase crystallization closest to the liquidus. When a compilation of >6500 igneous rocks from the Cascades and Sierra Nevada are compared to these experimental liquid lines of descent from this study, the lowest pressure liquids (400 MPa) are the most similar to those found in the North American arc environments. This suggests that plagioclase accompanies mafic silicates over a large range of the crystallization path for calc-alkaline liquids, which is only possible if the majority of differentiation of arc magmas occurs in the mid-to upper crust potentially along with open system processes. Therefore, reverse fractional crystallizations calculations for calc-alkaline primitive liquids that approximate their crystallization path by adding a combination of plagioclase and mafic silicate(s) back to the melt (as was done in the recalculation for the primitive liquids in Section 3 of this paper) are a reasonable approximation.

A recent model published by Kimura & Ariskin (2014) includes a subroutine (COMAGMAT3.72) that calculates basalt crystal fractionation paths in the presence of modest amounts of water (0.5, 1.0, 1.5, 2.0, 2.5, and 3.0 wt% H_2O). Rather than correcting the primitive melt by adding back the crystallized phases, this model starts with a provisional primary melt and fractionally crystallizes it along a predetermined liquid line of descent based on the experimental results of Tatsumi & Suzuki (2009) and then corrects the primary melt composition until the calculated fractionated melt matches the observed primitive melt. This model is likely suitable for crystallization of tholeiitic basalts with similar compositions, water contents (<3 wt% H_2O), crystallization pressures (3 kbars) and oxygen fugacities (NNO+2.5-3) to the study of Tatsumi and Suzuki (2009). The model has yet to be tested against experimental data on the liquid line of descent for other primitive arc magma compositions and for crystallization at other conditions.

The approach taken for the new reverse fractionation calculations presented for a diversity of primitive arc liquids in Section 3 does not so much aim to reverse the liquid line of descent step-by-step, one fractionating mineral assemblage at a time, but rather to approximate the bulk solid extract removed from the liquid using the pseudo-ternary projections, the mantle saturation points for the appropriate residue mineralogy, and the erupted volcanic rock mineralogy. The ability to identify the sequential crystallizing assemblages to reconstruct the fractionation path systematically for different primary arc magma compositions at a range of pressures, temperatures, H_2O contents, and fO_2s remains a goal to strive for in the future, as it is dependent on additional experimental studies like Blatter et al. (2013), a detailed review of all experimental arc liquid fractionation studies to date, and future studies of natural primitive arc magmas that measure mineral compositions, H_2O, and fO_2 in detail.

2. Considerations for Calculating Pressure and Temperature Using Primary Magma Compositions

a) Thermometer & Barometer Comparison

In order to assess the spread in the temperatures in the literature compilation in Figure 1 attributable to the use of different thermometers, mantle-equilibration temperatures are calculated for four primitive arc magmas using a range of models (Figure S4; Table S2). The samples include two arc basalts – one tholeiite ("82-72f" from Medicine Lake: Bartels et al. 1991) and one that lies in the calc-alkaline field ("83-43" from Mt Shasta: Baker et al. 1994) – as well as a high-Mg andesite ("TGI" from Japan: Tatsumi et al. 1981) and a boninite ("HCB Tonga 2" from Tonga: Falloon & Danyushevsky 2000). Prior to use in the thermometers, the arc

tholeiite and calc-alkaline basalt whole rock compositions were returned to equilibration with a mantle lherzolite for both olivine or olivine + plagioclase fractionation following the methods discussed in Section 3a of the main text. No correction was applied to the boninite and high-Mg andesite bulk rock compositions. Forward models, such as pMELTS (Ghiorso et al. 2002) and Arc Basalt Simulator (Kimura et al. 2009; 2014) were used by several studies but are not included in this comparison of thermometers because of the challenge of providing a direct comparison to the other thermometers given the range of possible input variables. The bulk of the rock compositions in this review are similar to the two arc basalts, therefore they provide a good comparison of the thermobarometers. All the thermometers compared produce temperature estimates within 86°C of one another for the calc-alkaline basalt (83-43) and 112°C for the tholeiite (82-72f) when an olivine-only fractionation correction is used and the sample is assumed to be dry. If the Ford et al. (1983) thermometer is excluded, which has errors of 130°C and is only used by one study included in Figure 1, this range drops to 40°C and 75°C, respectively. The thermometers vary by 42°C for the calc-alkaline basalt and 34°C for the tholeiite when an olivine+plagioclase fractionation correction is used and Ford et al. (1983) is excluded (see Table S2 for the total spread of temperatures with other assumptions).

Similarly, three of the most popular barometers are compared in Table S3 and the difference between them when all other variables are held constant is on average 2.6 kbars but can be as large as 4.9 kbars. These variations are smaller than the effect of different fractionation corrections, which can cause variations in the calculated pressure for the same sample of up to 10-13 kbar. In addition, the recalibration of the Beattie (1993) a^{liq}_{SiO2} barometer by Putirka (2008) produces similar results to the Lee et al. (2009) barometer but is more precise

at higher pressures (for more on the comparison to the Lee et al. (2009) model, see Putirka (2012)).

b) Recommended Thermobarometers

The Till et al. (2012a) thermobarometer for plagioclase and spinel lherzolite and Grove et al. (2013) thermobarometer for garnet lherzolite can be combined to predict the temperature and pressure of a melt in each of the lherzolite facies using an internally consistent set of equations that include the effect of H_2O with the smallest errors. These models can also be used to predict the melt composition produced by melting of peridotite if pressure and the peridotite source composition are specified (e.g., Behn and Grove, 2015). Now with the addition of Mitchell and Grove (2015) to this system of equations, it provides the additional benefit of being able to vary the residue composition at very low errors (mean absolute error of Mitchell and Grove thermometer is 25°C).

3. Worked Example

In the recalculations discussed in Section 3 of the main paper, the essential approach is to divide the calculations into three parts: 1) reversing the effects of fractional crystallization to the point that Fe/Mg is appropriate for mantle olivine, 2) iterating step 1, adjusting the phase proportions to obtain a match wherein the reverse-fractionated liquid compositions are similar to lherzolite- or harzburgite-saturated liquids and 3) estimating the pressure and temperature of that saturation calculated for plagioclase and spinel lherzolite using the equations of Till et al. (2012a), garnet lherzolite with Grove et al. (2013), or harzburgite using Mitchell and Grove (2015). This approach has been successfully applied to nominally anhydrous primitive basalts

erupted in arcs (e.g., Till et al. 2013) and other tectonic setting such as flood basalts (e.g., Chatterjee and Sheth 2015).

The following section walks through these specific methods to correct a primitive basalt composition for fractional crystallization following the methods of Yang et al. (1996) and then using this primary magma composition to calculate the pressure and temperature it was last in equilibrium with the lherzolitic mantle using the thermometers and barometers of Till et al. (2012a) and Grove et al. (2013).

a) Sample Information & Previous Studies

This demonstration utilizes primitive arc basalt STV-301 (47 wt% SiO_2, Mg#=0.71) from Soufriere Volcano on St. Vincent island in the Lesser Antilles arc. The composition, petrography, mineralogy, likely fractionation path and a model for magma genesis of this arc basalt were published by Heath et al. (1998). Heath et al. (1998) determined formation conditions of 1030-1130°C at QFM+1.5 based on the olivine-spinel thermometer of Ballhaus et al. (1991) at depths of ~17 kbars based on a comparison of the basalt to experimental phase equilibria. Pichavant et al. (2002) experimentally investigated the phase relations of the basalt and Bouvier et al. (2008) conducted ion probe analyses of olivine-hosted melt inclusions from this basalt. Pichavant et al. (2002) experimentally-determined mantle equilibration conditions for this basalt of 1235°C at 11.5 kbar.

b) Fractional Crystallization Correction

In order to return STV-301 to a primary magma composition, the sample must first be adjusted for crystallization upon ascent. Health et al. (1998) report that arc basalt STV-301 contains 67.7% olivine + 13% oxides + 19.1 % clinopyroxene + trace plagioclase phenocrysts.

H_2O measured by ion microprobe of olivine-hosted melt inclusions corrected for post-entrapment crystallization suggest pre-eruptive H_2O contents of 2.4-3.2 wt. % (Bouvier et al. 2008). It is likely that the H_2O contents were originally higher due to propensity for diffusive loss of H through olivine, however here we use ion microprobe measured H_2O contents.

To assess both the appropriate phases to add back to the liquid and evaluate the success of a trial fractionation correction, the sample is plotted on plag-cpx-oliv, oliv-plag-qtz and oliv-cpx-qtz ternary diagrams using oxygen units following the pseudo-quaternary projection scheme of Tormey et al. (1987) with the correction of Grove et al. (1993) (Fig. S5). Also plotted on these diagrams for comparison are the plagioclase, spinel and garnet lherzolite mantle multiple saturation points calculated for STV-301. The equations to calculate the mantle lherzolite multiple saturation points for a primitive basalt of interest are from Till et al. (2012) and Grove et al. (2013). A reverse fractionation calculation consistent with the sample mineralogy should ideally return the liquid to equilibrium with the mantle as indicated by the liquid plotting on the same mantle multiple saturation point in all three ternary projections and being in equilibrium with a specified mantle olivine composition (taken here to be Fo90). An excel spreadsheet that plots a primitive magma composition and the lherzolite multiple saturation points in ternary space following these methods is available as an electronic supplementary file ("fracest.xls").

To correct the liquid composition for crystallization, the MORB fractionation model of Grove et al., (1992) updated by Yang et al. (1996) is employed. Equations from Yang et al. (1996) can be programed into a relative simple program in excel, MATLAB or similar, where the user specifies the major oxide composition of the primitive arc basalt of interest, the abundance of the various mineral phases to add back in (or subtract from the liquid to model fractional crystallization), and a suite of partition coefficients. The program then adds the

specified proportion of the mineral phases back to the liquid in increments of 1 wt%. Given the mineralogy of STV-301, 100% olivine was added back to the liquid using a $K_D^{Fe\text{-}Mg}{}_{oliv\text{-}liquid}$ of 0.3 for three steps (equivalent 3% crystal addition), followed by 1% crystal addition of 70% olivine and 30% clinopyroxene. Following this fractional crystallization calculation, the corrected primary liquid for STV-301 has an Mg# of 0.73 such that it is in equilibrium with Fo90 mantle olivine and plots on the 19 kilobar multiple saturation point for spinel lherzolite in all three ternary projections in Figure S5. Thus it is deemed the reverse crystallization calculation is successful (Table S4). If the liquid did not plot on the same mantle multiple saturation point in all three projections following the crystallization correction, an alternative proportion of phases would be tried until this criteria was met. If plagioclase were included in the fractionation calculation, the Ca-Na partition coefficient between plagioclase and liquid would be adjusted for the H_2O content of the sample (here ~2.5 wt% H_2O such that K_D Ca-Na plag-liquid = 1.7; Sisson and Grove, 1993). Clinopyroxene partition coefficients can also be adjusted based on H_2O contents using the experimental data from studies such as Grove et al. (2003) and Gaetani and Grove (1998).

Table S4. Comparison of STV-301 composition before and after the reverse fractionation calculation.

	SiO_2	**TiO_2**	**Al_2O_3**	**FeO***	**MnO**	**MgO**	**CaO**	**Na_2O**	**K_2O**
STV-301 whole rock composition	47.01	1.07	15.28	8.79	0.16	12.5	10.96	2.23	0.47

STV-301 calculated primary liquid	47.6	1.05	15.06	8.94	0.16	13.7	2.19	2.19	0.46

c) P-T Calculations

The primary liquid composition can then be used with the equations of Till et al. (2012a) (see their Table 5) to calculate the pressure and temperature it was in equilibrium with a spinel lherzolite residue. If the corrected primary liquid instead plotted on a plagioclase lherzolite multiple saturation point, the plagioclase lherzolite thermometer and barometer of Till et al. (2012a) should be employed, or in the case of equilibrium with garnet lherzolite, the garnet lherzolite thermometer and barometer of Grove et al. (2013) (see their Table 4). If the fractionation-corrected liquid is in equilibrium with mantle olivine but does not plot in proximity to any lherzolite multiple saturation points, the liquid likely did not result from melting a lherzolitic residue and instead may be in equilibrium with a mantle harzburgite like the primitive high-Mg andesites reviewed in this study. Such liquids should be dealt with in accordance with the approach illustrated in Mitchell and Grove (2015). Alternatively, fractionation-corrected liquids that don't align with lherzolite or harzburgite multiple saturation points at any pressure may be the result of pyroxenite melting, or mantle melting in the presence of significant quantities of CO_2, both of which are illustrated and discussed in Grove et al. (2013).

The independent variables in the Till et al. (2012a) barometer are the olivine mineral component, 1-Mg#, NaK#, TiO_2 (wt%) and K_2O (wt%) for the primary liquid. These variables were selected after extensive testing and principle component analyses, as they vary systematically in experiments as result of changes in the pressure of mantle melting. The wt%

oxides for the primary liquid composition of interest can be converted to the pseudo-quaternary mineral components Olivine, Clinopyroxene, Plagioclase and Quartz using the method of Tormey et al. (1987) with the correction of Grove (1993) (this is the same scheme that was used to plot the liquids in pseudo-quaternary space to evaluate the fractional crystallization correction). NaK# can be calculated using the primary liquid oxide wt% in the following equation: NaK#=(Na_2O+K_2O)/ (Na_2O+K_2O+CaO). The thermometer of Till et al. (2012a) uses the same independent variables as the barometer with the exception of using pressure (in GPa) in place of the olivine mineral component value. The thermometer and barometer return the temperature and pressure of the primary magma's last equilibration with a lherzolitic mantle in units of °C and GPa. The average absolute error on both the plagioclase and spinel lherzolite thermometers is 11°C. The spinel lherzolite barometer has an error of 0.15 GPa (1.5 kilobars, ~4.5 km depth) and the plagioclase lherzolite barometer 0.08 GPa (0.8 kilobars, ~2.4 km).

The spinel lherzolite thermometer and barometer return anhydrous mantle equilibration conditions for the calculated STV-301 primary liquid of 1392°C and 18.5 kbars.

d) H_2O Correction of Mantle Pressure & Temperature

The temperatures and pressures returned by the Till et al. (2012a) thermometer and barometer reflect the conditions of mantle equilibration under nominally anhydrous conditions (≤1 wt% H_2O). Because ion microprobe analyses of olivine-melted inclusions in STV-301 suggest pre-eruptive H_2O contents of ≥2.5 wt% H_2O, there is one more step to correct the anhydrous mantle equilibration conditions for the effect of H_2O. Till et al. (2012a) Figure 7 presents linear equations that calculate how much the mantle equilibration temperature is lowered and the mantle equilibration pressure increased by a given primary magmatic H_2O content. These H_2O corrections are based on the limited experimental dataset published to date

on the behavior of liquids in equilibrium with the mantle at H_2O-undersaturated conditions. When 2.5 wt% H_2O is used, the mantle equilibration temperature drops 67°C and the equilibration pressure increases 0.6 kbars. This yields mantle equilibration conditions for the STV-301 calculated primary liquid of 1392°C and 19.1 kbars. This pressure and temperature for the STV-301 primary liquid is included in Figure 7 in the main text as one of the "tholeiitic basalt" samples.

References Cited

Baker, M., Grove, T.L., and Price, R. (1994) Primitive Basalts and Andesites From the Mt Shasta Region, N California - Products of Varying Melt Fraction and Water-Content. Contributions to Mineralogy and Petrology, 118, 111–129.

Bartels, K.S., Kinzler, R.J., and Grove, T.L. (1991) High pressure phase relations of primitive high-alumina basalts from Medicine Lake volcano, northern California. Contributions to Mineralogy and Petrology, 108, 253–270.

Beattie, P. (1993) Olivine-melt and orthopyroxene-melt equilibria. Contributions to Mineralogy and Petrology, 115, 103–111.

Behn, M.D., and Grove, T.L. (2015) Melting systematics in mid-ocean ridge basalts: Application of a plagioclase-spinel melting model to global variations in major element chemistry and crustal thickness. Journal of Geophysical Research-Solid Earth, 120, 4863–4886.

Blatter, D.L., Sisson, T.W., and Hankins, W.B. (2013) Crystallization of oxidized, moderately hydrous arc basalt at mid- to lower-crustal pressures: implications for andesite genesis. Contributions to Mineralogy and Petrology, 166, 861–886.

Bouvier, A.S., Metrich, N., and Deloule, E. (2008) Slab-Derived Fluids in the Magma Sources of St. Vincent (Lesser Antilles Arc): Volatile and Light Element Imprints. Journal of Petrology, 49, 1427–1448.

Chatterjee, N., and Sheth, H. (2015) Origin of the Powai ankaramite, and the composition, P–T conditions of equilibration and evolution of the primary magmas of the Deccan tholeiites. Contributions to Mineralogy and Petrology, 169, 32–24.

Falloon, T., and Danyushevsky, L. (2000) Melting of refractory mantle at 1.5, 2 and 2.5 GPa under, anhydrous and H2O-undersaturated conditions: Implications for the petrogenesis of high-Ca boninites and the influence of subduction components on mantle melting. Journal of Petrology, 41, 257–283.

Ford, C.E., Russell, D.G., Craven, J.A., and Fisk, M.R. (1983) Olivine Liquid Equilibria - Temperature, Pressure and Composition Dependence of the Crystal Liquid Cation Partition-Coefficients for Mg, Fe-2+, Ca and Mn. Journal of Petrology, 24, 256–265.

Ghiorso, M.S., Hirschmann, M.M., Reiners, P.W., and Kress, V.C., III (2002) The pMELTS: A revision of MELTS for improved calculation of phase relations and major element partitioning related to partial melting of the mantle to 3 GPa. Geochem Geophys Geosyst, 3, 1–35.

Green, D.H., Falloon, T.J., and Taylor, W.R. (1987) Mantle-derived magmas: Roles of variable source peridotite and variable CHO fluid compositions. In B.O. Mysen, Ed., Magmatic Processes: Physiochemical Principles. Geochem. Soc.

Grove, T.L. (1993) Corrections to expressions for calculating mineral components in "Origin of Calc-Alkaline Series Lavas at Medicine Lake Volcano by Fractionation, Assimilation and Mixing" and “Experimental Petrology of normal MORB near Kane Fracture Zone: 22°-25°N, mid-Atlantic ridge.” Contributions to Mineralogy and Petrology, 114, 422–424.

Grove, T.L., Holbig, E.S., Barr, J.A., Till, C.B., and Krawczynski, M.J. (2013) Melts of garnet lherzolite: experiments, models and comparison to melts of pyroxenite and carbonated lherzolite. Contributions to Mineralogy and Petrology, 166, 887–910.

Grove, T.L., Kinzler, R.J., and Bryan, W.B. (1992) Fractionation of Mid-Ocean Ridge Basalt (MORB). In Mantle Flow and Melt Generation at Mid-Ocean Ridges Vol. 71, pp. 281–310. American Geophysical Union.

Heath, E., Macdonald, R., and Belkin, H. (1998) Magmagenesis at Soufriere Volcano, St Vincent, Lesser Antilles Arc. Journal of Petrology.

Herzberg, C., and Asimow, P.D. (2008) Petrology of some oceanic island basalts: PRIMELT2.XLS software for primary magma calculation. Geochem Geophys Geosyst, 9.

Jayasuriya, K., O’Neill, H. St., Berry, A.J., and Campbell, S.J. (2004) A Mössbauer study of the oxidation state of Fe in silicate melts. American Mineralogist, 89, 1597–1609.

Kelemen, P.B., Shimizu, N., and SALTERS, V. (1995) Extraction of Mid-Ocean-Ridge Basalt From the Upwelling Mantle by Focused Flow of Melt in Dunite Channels. Nature, 375, 747–753.

Kelemen, P.B., Whitehead, J.A., Aharonov, E., and Jordahl, K.A. (1995) Experiments on flow focusing in soluble porous media, with applications to melt extraction from the mantle. Journal of Geophysical Research, 100, 475–496.

Kimura, J.-I., and Ariskin, A.A. (2014) Calculation of water-bearing primary basalt and estimation of source mantle conditions beneath arcs: PRIMACALC2 model for WINDOWS. Geochem Geophys Geosyst, 15, 1494–1514.

Kimura, J.-I., Hacker, B.R., van Keken, P.E., Kawabata, H., Yoshida, T., and Stern, R.J. (2009) Arc Basalt Simulator version 2, a simulation for slab dehydration and fluid-fluxed mantle melting for arc basalts: Modeling scheme and application. Geochem Geophys Geosyst, 10, n/a–n/a.

Kress, V.C., and Carmichael, I.S. (1991) The compressibility of silicate liquids containing Fe2O3 and the effect of composition, temperature, oxygen fugacity and pressure on their redox states. Contributions to Mineralogy and Petrology, 108, 82–92.

Lee, C.-T.A., Luffi, P., Plank, T., Dalton, H., and Leeman, W.P. (2009) Constraints on the depths and temperatures of basaltic magma generation on Earth and other terrestrial planets using new thermobarometers for mafic magmas. Earth and Planetary Science Letters, 279, 20–33.

Mandler, B.E., Donnelly-Nolan, J.M., and Grove, T.L. (2014) Straddling the tholeiitic/calc-alkaline transition: the effects of modest amounts of water on magmatic differentiation at Newberry Volcano, Oregon. Contributions to Mineralogy and Petrology, 168, 1–25.

Matzen, A.K., Baker, M.B., Beckett, J.R., and Stolper, E.M. (2011) Fe-Mg Partitioning between Olivine and High-magnesian Melts and the Nature of Hawaiian Parental Liquids. Journal of Petrology, 52, 1243–1263.

Mitchell, A.L., and Grove, T.L. (2015) Melting the hydrous, subarc mantle: the origin of primitive andesites. Contributions to Mineralogy and Petrology, 170, 1–23.

Mitchell, A.L. and Grove, T.L. (in press) Experiments on melt-rock reaction in the mantle wedge. Contributions to Mineralogy and Petrology.

Morishita T. Dilek Y., Shallo M., Tamura A., Arai S. (2011) Insight into the uppermost mantle section of a maturing arc: the Eastern Mirdita ophiolite, Albania. Lithos 124, 215–226.

Mysen, B.O., and Boettcher, A.L. (1975) Melting of a Hydrous Mantle 1. Phase Relations of Natural Peridotite at High-Pressures and Temperatures with Controlled Activities of Water, Carbon-Dioxide, and Hydrogen. Journal of Petrology, 16, 520–548.

Parman, S.W., Grove, T.L., Kelley, K.A., and Plank, T. (2011) Along-Arc Variations in the Pre-Eruptive H2O Contents of Mariana Arc Magmas Inferred from Fractionation Paths. Journal of Petrology, 52, 257–278.

Pearce J.A., Parkinson I.J. (1993) Trace element models for mantle melt- ing: application to volcanic arc petrogenesis. In: Prichard HM, Alabaster T, Harris NBW, Neary CR (eds.) Magmatic processes and plate tectonics. Geological Society, London, Special Publication, 76, 373–403.

Pichavant, M., and Macdonald, R. (2007) Crystallization of primitive basaltic magmas at crustal pressures and genesis of the calc-alkaline igneous suite: experimental evidence from St Vincent, Lesser Antilles arc. Contributions to Mineralogy and Petrology, 154, 535–558.

Pirard C., Hermann J, O'Neill H.St.C. (2013) Petrology and geochemis- try of the crust-mantle boundary in a nascent arc, Massif du Sud ophiolite, New Caledonia, SW Pacific. Journal Petrology 54, 1759–1792.

Pirard, C., and Hermann, J. (2015) Focused fluid transfer through the mantle above subduction zones. Geology, 43, 915–918.

Putirka, K. (2012) Cenozoic volcanism in the Sierra Nevada and Walker Lane, California, and a new model for lithosphere degradation. Geosphere, 8, 265.

Putirka, K. (2016) Rates and styles of planetary cooling on Earth, Moon, Mars, and Vesta, using new models for oxygen fugacity, ferric-ferrous ratios, olivine-liquid Fe-Mg exchange, and mantle potential temperature. American Mineralogist, 101, 819–840.

Sisson, T.W., and Grove, T.L. (1993) Experimental Investigations of the Role of H2O in Calc-Alkaline Differentiation and Subduction Zone Magmatism. Contributions to Mineralogy and Petrology, 113, 143–166.

Tatsumi, Y., and Suzuki, T. (2009) Tholeiitic vs Calc-alkalic Differentiation and Evolution of Arc Crust: Constraints from Melting Experiments on a Basalt from the Izu-Bonin-Mariana Arc. Journal of Petrology, 50, 1575–1603.

Till, C.B., Grove, T.L., and Krawczynski, M.J. (2012) A melting model for variably depleted and enriched lherzolite in the plagioclase and spinel stability fields. Journal of Geophysical Research, 117.

Till, C.B., Grove, T.L., Carlson, R.W., Fouch, M.J., Donnelly-Nolan, J.M., Wagner, L.S., and Hart, W.K. (2013) Depths and temperatures of <10.5 Ma mantle melting and the lithosphere-asthenosphere boundary below southern Oregon and northern California. Geochem Geophys Geosyst, 15, 864–879.

Toplis, M.J. (2005) The thermodynamics of iron and magnesium partitioning between olivine and liquid: criteria for assessing and predicting equilibrium in natural and experimental systems. Contributions to Mineralogy and Petrology, 149, 22–39.

Tormey, D.R., Grove, T.L., and Bryan, W.B. (1987) Experimental petrology of normal MORB near the Kane Fracture Zone: 22°-25° N, mid-Atlantic ridge. Contributions to Mineralogy and Petrology, 96, 121–139.

Umino, S., & Kushiro, I. (1989). Experimental studies on boninite petrogenesis. *Boninites and Related Rocks. Unwin Hyman, London*, 89-111.

Wagner, T.P., Donnelly-Nolan, J.M., and Grove, T.L. (1995) Evidence of hydrous differentiation and crystal accumulation in the low-MgO, high-Al2O3 Lake Basalt from Medicine Lake volcano, California. Contributions to Mineralogy and Petrology, 121, 201–216.

Wang, C., Liang, Y., Dygert, N., and Xu, W. (2016) Formation of orthopyroxenite by reaction between peridotite and hydrous basaltic melt: an experimental study. Contributions to Mineralogy and Petrology, 171, 1–18.

Yang, H.J., Kinzler, R.J., and Grove, T.L. (1996) Experiments and models of anhydrous, basaltic olivine-plagioclase-augite saturated melts from 0.001 to 10 kbar. Contributions to Mineralogy and Petrology.

Supplementary Figure Captions:

Figure S1. Pseudo-ternary projections depicting the compositions of the tholeiitic and calc-alkaline basalts (a), primitive andesites (b) and high MgO arc magmas (c) chosen for the pressure and temperature recalculations prior to fractional crystallization corrections. This is the same data as in Figure 4 of the main text with three different projections shown instead of just one, along with the location of a melt in equilibrium with plagioclase (blue y's), spinel (green y's) and garnet (red y's) lherzolite, also known as the lherzolite "multiple saturation points", over a range of pressures from Till et al. (2012a) and Grove et al. (2014). The calc-alkaline and tholeiitic primary liquids in (a) relatively silica undersaturated compared to primitive high-Mg andesites and high MgO primitive lavas, such as boninites and picrites. High MgO primitive arc magmas from GEOROC not in the P-T recalculations are also shown in panel 10c (black circles) to illustrate the full diversity of high MgO liquid compositions. The location of the lherzolite multiple saturation points are shown for the oliv-plag-qtz ternary to illustrate how the high MgO samples are either the result of harzburgite melting or lherzolite melts reacting with harzburgite upon ascent. Overall both the liquid types in (b) & (c) are relatively silica-staturated compared to the more typical arc basalts shown in a) due to their being in equilibrium with a mantle harz-burgite rather than lherzolite.

Figure S2. **Pseudo-ternary projection showing the schematic location of primitive arc liquids in equilibrium with different types of mantle residues found at arcs based on experiments and investigations of natural samples.** Liquids in equilibrium with lherzolite based on the work of Till et al. (2012a, 2013). Liquids in equilibrium with harzburgite based on the work of Mitchell and Grove (2015) and liquids in equilibrium with dunite based on the work of Mitchell and Grove (in press).

Figure S3. **Experimentally determined liquid lines of descent for primitive arc magmas compared to arc melt inclusions and primitive magmas in the literature compilation**. Plot of composition of the samples in this review (color coding as in main text Figure 1) compared to a database of melt inclusion compositions from arcs (gray diamonds), experimentally determined liquid lines of descent for primitive arc magmas (colored lines) and the calc-alkaline vs. tholeiitic fields of Miyashiro (1974). Melt inclusion compositions were downloaded from the 2014 version of the GEOROC melt inclusion database and filtered for those erupted at arcs. Liquid lines of descent are from the studies of Grove and Baker (1984), Grove and Kinzler (1986), Juster et al. (1989), Sisson and Grove (1993), Wagner et al. (1995), Grove et al. (2003), Hamada and Fuji (2008), Blatter et al. (2013), and Mandler et al. (2014). Also shown for reference are the composition of low degree melt of a spinel lherzolite with 6 wt. % H_2O (Gaetani and Grove, 1998) and garnet lherzolite with 14 wt% H_2O (Till et al., 2012a).

Figure S4. Comparison of thermometers used in the literature compilation. Temperature estimates shown are all using the same pressure estimate, with the exception of experiments, where the experimental pressure was adopted for the thermometry calculations (1.2 GPa for the calc-alkaline basalt; 1.3 GPa for the tholeiitic basalt; 1.5 GPa for the high Mg-andesite and boninite). Errors for each thermometer are illustrated as the standard error reported by the evaluation of Putirka (2008), or that reported in original reference if not included in the comparison of Putirka (2008). No reverse fractionation calculations are required for the boninites and high-Mg andesites. The tholeiites are adjusted back to equilibrium with Fo90 mantle olivine with the chosen fractionating assemblage. Squares denote the average temperature

and standard deviation produced by the various thermometers for each set of conditions. Where H_2O in included in the calculation, the error bars, averages and standard deviations are shown in blue.

Figure S5. **Pseudo-ternary for the worked example**. Pseudo-ternary projections depicting the bulk composition of STV-301 (prior to fractional crystallization correction) in red, and the fractional crystallization corrected liquid in green. These are shown along with the location of a melt in equilibrium with plagioclase (blue y's), spinel (green y's) and garnet (red y's) lherzolite, also known as the lherzolite "multiple saturation points", over a range of pressures from Till et al. (2012) and Grove et al. (2014). Note that the STV-301 primary liquid composition (green square) plots on the spinel lherzolite 19 kilobar multiple saturation point in all three projections.

Table S1. All literature sample compositions and associated pressure-temperature estimates illustrated in Figure 1.

Table S2. **Comparison of the results of three popular mantle liquid thermometers.**

Table S3. Comparison of the results of three popular mantle liquid barometers.

Table S4. Comparison of STV-301 composition before and after the reverse fractionation calculation.

Supplemental Ternary Projection Tool. Spreadsheet for plotting major element compositions in pseudo-ternary projection space and the calculation of the mantle multiple saturation points for plagioclase, spinel and garnet lherzolite from Till et al., (2012a) and Grove et al.,(2013). The major element composition of primitive magma of interest should be typed into the yellow cells in the first row. Multiple saturation points for this composition will be calculated and plotted on the ternary diagrams by the colored symbols and the sample composition plotted by the red box. If additional sample compositions are typed into the cells below, they will be plotted below but note the multiple saturation points are only calculated for the composition in the top row with yellow cells.

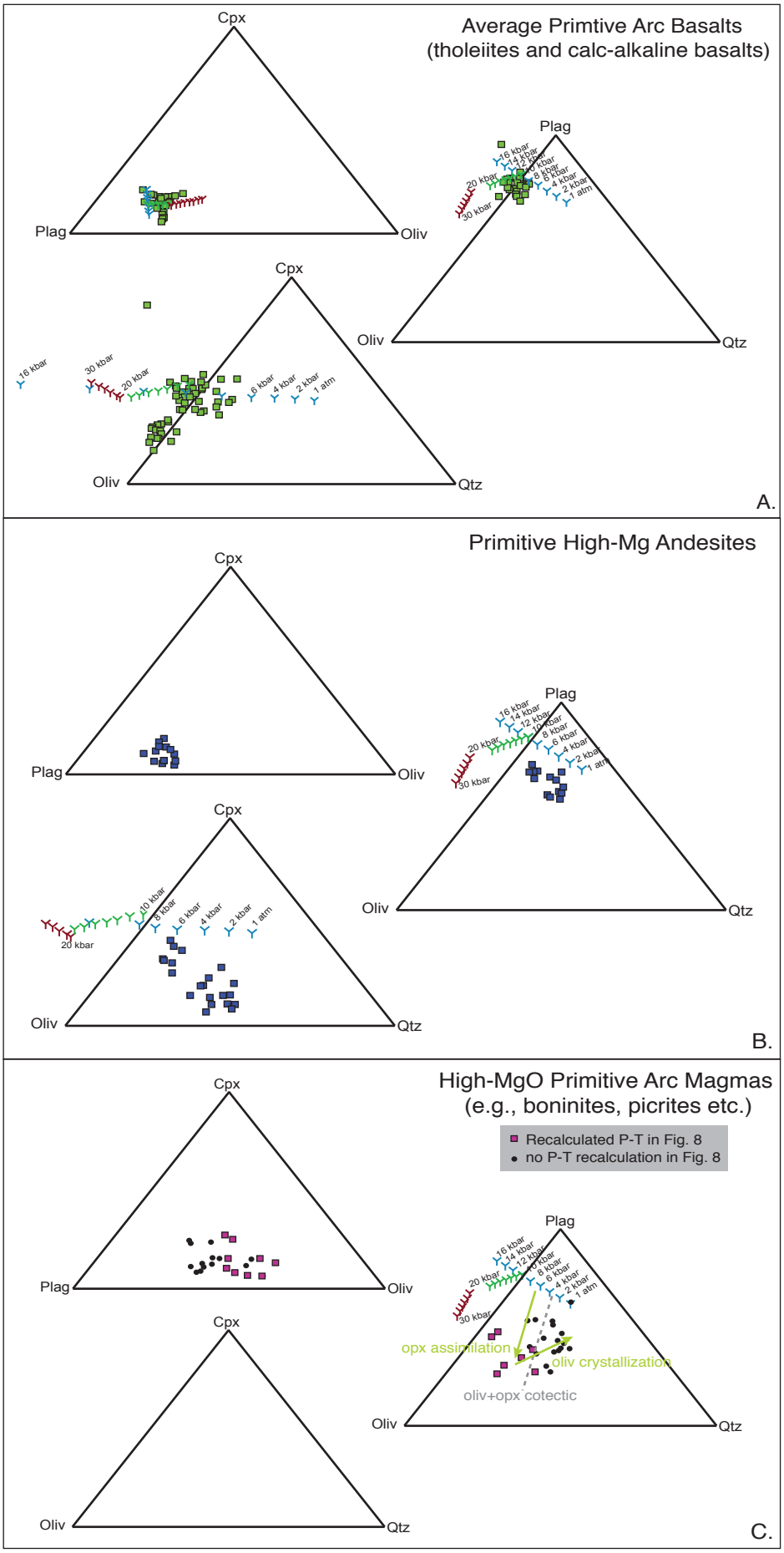
Average Primtive Arc Basalts
(tholeiites and calc-alkaline basalts)
Cpx
Plag
Oliv
Plag
Oliv
Qtz
Cpx
Oliv
Qtz
16 kbar
30 kbar
20 kbar
16 kbar
14 kbar
12 kbar
10 kbar
8 kbar
6 kbar
4 kbar
2 kbar
1 atm
A.
Primitive High-Mg Andesites
Cpx
Plag
Oliv
Plag
Oliv
Qtz
Cpx
Oliv
Qtz
20 kbar
10 kbar
8 kbar
6 kbar
4 kbar
2 kbar
1 atm
B.
High-MgO Primitive Arc Magmas
(e.g., boninites, picrites etc.)
Recalculated P-T in Fig. 8
no P-T recalculation in Fig. 8
Cpx
Plag
Oliv
Plag
Oliv
Qtz
Cpx
Oliv
Qtz
opx assimilation
oliv crystallization
oliv+opx cotectic
C.

Figure S1.

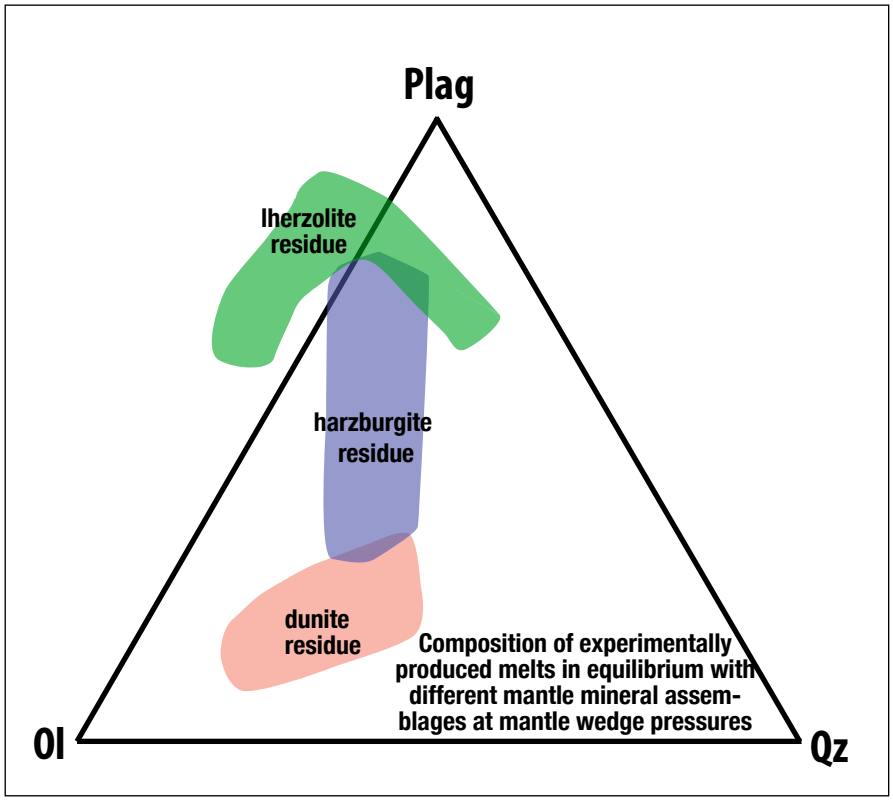
Plag
lherzolite residue
harzburgite residue
dunite residue
Composition of experimentally produced melts in equilibrium with different mantle mineral assemblages at mantle wedge pressures
Ol
Qz

Figure S2.

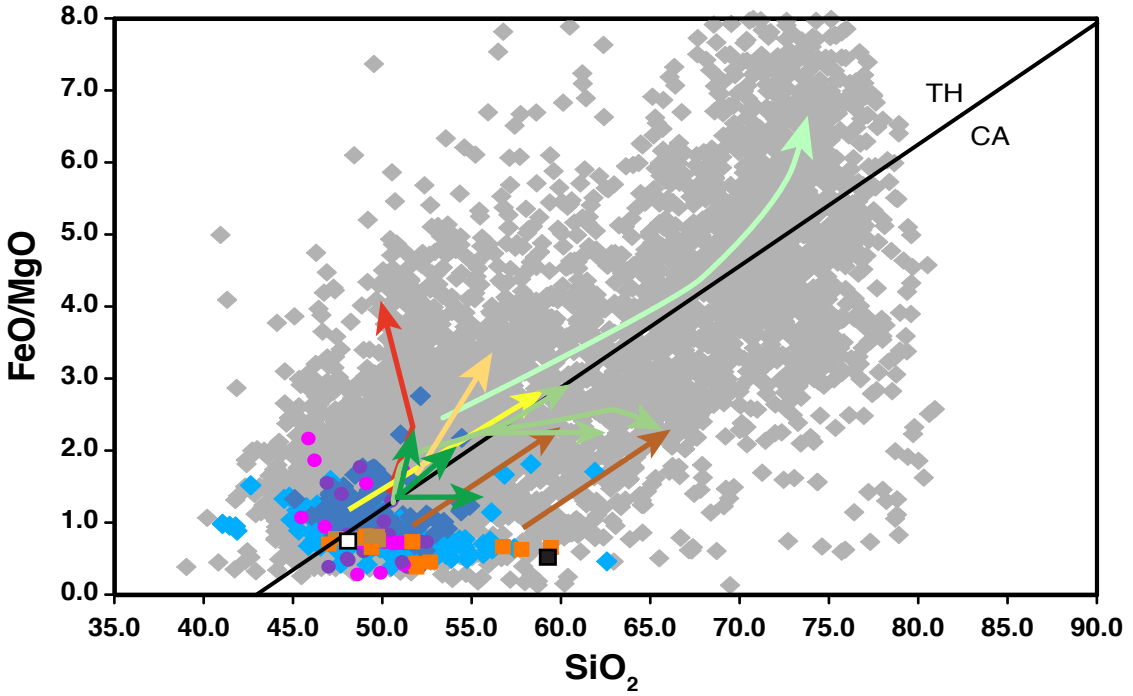
8.0
7.0
6.0
5.0
4.0
3.0
2.0
1.0
0.0
FeO/MgO
35.0
40.0
45.0
50.0
55.0
60.0
65.0
70.0
75.0
80.0
85.0
90.0
SiO2
TH
CA

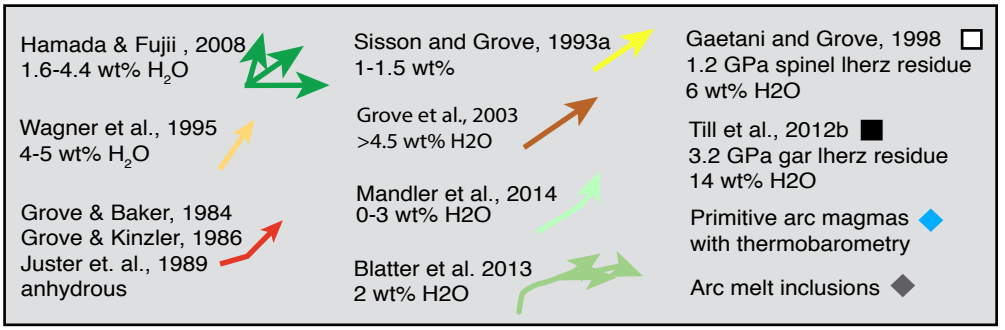
Hamada & Fujii , 2008
1.6-4.4 wt% H2O
Wagner et al., 1995
4-5 wt% H2O
Grove & Baker, 1984
Grove & Kinzler, 1986
Juster et. al., 1989
anhydrous
Sisson and Grove, 1993a
1-1.5 wt%
Grove et al., 2003
>4.5 wt% H2O
Mandler et al., 2014
0-3 wt% H2O
Blatter et al. 2013
2 wt% H2O
Gaetani and Grove, 1998
1.2 GPa spinel lherz residue
6 wt% H2O
Till et al., 2012b
3.2 GPa gar lherz residue
14 wt% H2O
Primitive arc magmas
with thermobarometry
Arc melt inclusions

Figure S3.

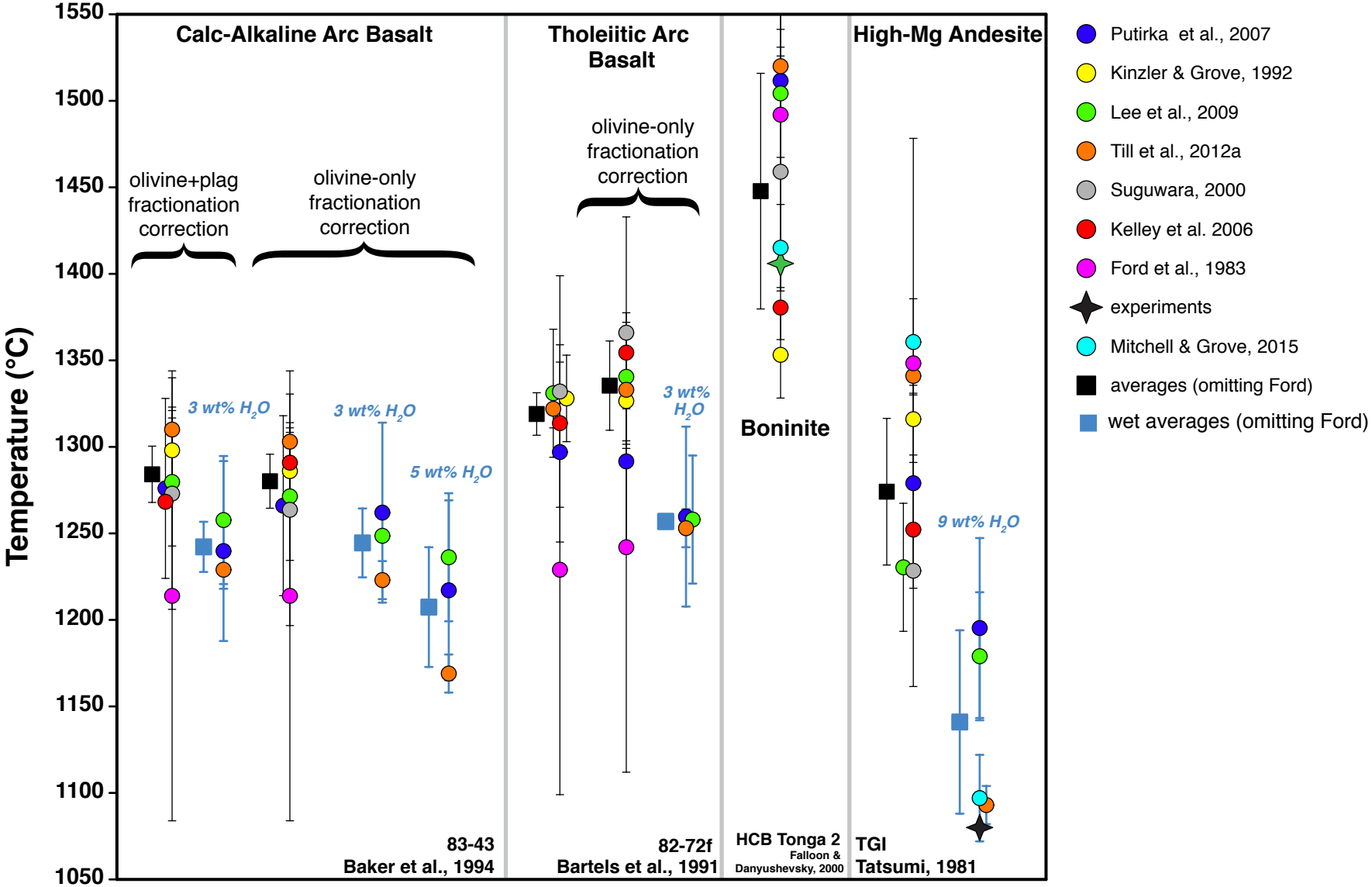
Calc-Alkaline Arc Basalt
Tholeiitic Arc Basalt
High-Mg Andesite
Temperature (°C)
1550
1500
1450
1400
1350
1300
1250
1200
1150
1100
1050
olivine+plag fractionation correction
olivine-only fractionation correction
olivine-only fractionation correction
3 wt% H2O
3 wt% H2O
5 wt% H2O
3 wt% H2O
9 wt% H2O
Boninite
83-43
Baker et al., 1994
82-72f
Bartels et al., 1991
HCB Tonga 2
Falloon & Danyushevsky, 2000
TGI
Tatsumi, 1981
Putirka et al., 2007
Kinzler & Grove, 1992
Lee et al., 2009
Till et al., 2012a
Suguwara, 2000
Kelley et al. 2006
Ford et al., 1983
experiments
Mitchell & Grove, 2015
averages (omitting Ford)
wet averages (omitting Ford)

Figure S4.

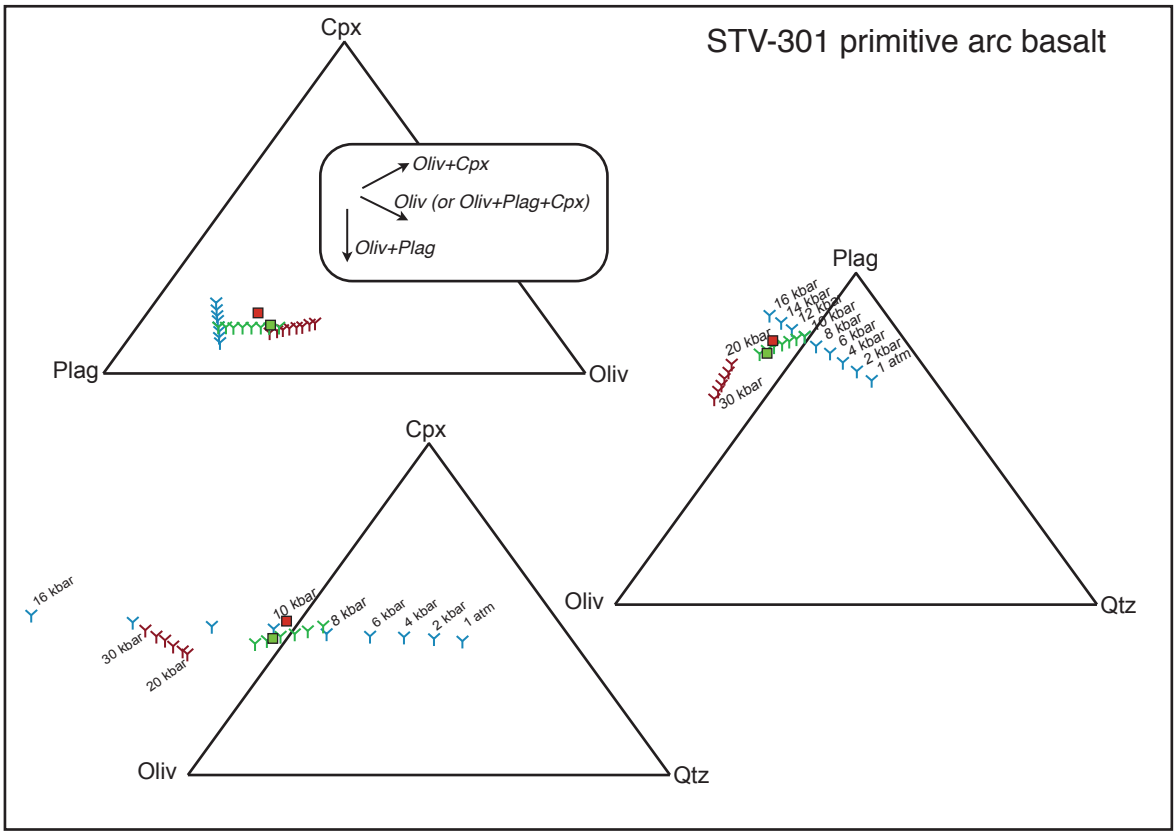
STV-301 primitive arc basalt
Cpx
Oliv+Cpx
Oliv (or Oliv+Plag+Cpx)
Oliv+Plag
Plag
Oliv
Plag
16 kbar
14 kbar
12 kbar
10 kbar
8 kbar
6 kbar
4 kbar
2 kbar
1 atm
20 kbar
30 kbar
Oliv
Qtz
Cpx
16 kbar
30 kbar
20 kbar
10 kbar
8 kbar
6 kbar
4 kbar
2 kbar
1 atm
Oliv
Qtz

Figure S5.